Received: 21 December 2023 | Revised: 6 June 2024 | Accepted: 8 September 2024

DOI: 10.1002/jcc.27505

RESEARCH ARTICLE

Journal of COMPUTATIONAL CHEMISTRY WILEY

Modulating the oxygen affinity of porphyrins with metals, ligands, and functional groups: A DFT study

Sebastian Ovalle | **Cecile Malardier-Jugroot**

Department of Chemistry and Chemical Engineering, Royal Military College of Canada, Kingston, Ontario, Canada

Correspondence
Cecile Malardier-Jugroot, Department of Chemistry and Chemical Engineering, Royal Military College of Canada, Kingston, ON, Canada.
Email: cecile.malardier-jugroot@rmc.ca

Funding information
Natural Sciences and Engineering Research Council of Canada

Abstract

The interaction between different metals (M), axial ligands (L), and ring substituents (R) in porphyrins was investigated using density functional theory. Different combinations of iron and cobalt as metal centers; imidazole, chlorine, and an n-heterocyclic carbene (NHC) as axial ligands, and unsubstituted, octaethyl-, and tetraphenyl-porphyrins were explored in their low, intermediate, and high-spin states, alongside oxygen affinity. Remarkably, the n-heterocyclic carbene enhanced the affinity of cobalt porphyrins to oxygen, with binding energies on average 4.4 kcal mol^{-1} higher than FeP with the same ligand, and 0.78 kcal mol^{-1} higher than FeP with imidazole. The planarity of the iron tetraphenyl porphyrin with imidazole compared to its ruffled cobalt counterpart is noteworthy in both oxy- and deoxy-forms, highlighting imidazole's stabilizing influence on the porphyrin structure, particularly iron porphyrins, alongside imidazole's stabilizing effect on the affinity to O_2. Despite the significant non-planarity induced by NHC as an axial ligand -regardless of the metal or ring substituent used-, it did not hinder the affinity of CoP to O_2 (14.26 kcal mol^{-1}, on average) as it did with the FeP with NHC (9.88 kcal mol^{-1}, on average). Cobalt porphyrins with n-heterocyclic carbene ligands show promising potential for O_2 activation or oxygen transport applications. The results show the complex interactions between the different parts of metalloporphyrins and highlight the capability of tailoring their affinity to O_2. It also exemplifies the stabilizing effect of imidazole on the porphyrins, providing a very narrow range of binding energies and smaller differences in their geometries.

KEYWORDS
cobalt, iron, n-heterocyclic carbene, oxygen binding, porphyrin

1 | INTRODUCTION

Metalloporphyrins are coordination compounds integral to various biological processes like respiration and photosynthesis. The heme prosthetic group, found in hemoglobin and myoglobin, plays a crucial role in oxygen transport and has been extensively studied. Hemoglobin consists of four sub-units, each housing a heme group. Oxygen binding occurs at the iron cation coordinated to the nitrogen atoms in the porphyrin ring.

The core of the heme group is a porphyrin ring, allowing the functionalization with diverse substituents like phenyl and alkyl groups.[1–3] The ferrous metal center adopts an octahedral coordination geometry, featuring four coordination sites for the nitrogen atoms within the porphyrin core and two axial sites.[4] In hemoglobin, one of these axial

sites hosts a histidine residue, leaving the sixth site available for binding dioxygen.[5]

Extensive research has explored the impact of various substituents, metals, and axial ligands on the properties of metalloporphyrins, including catalysis, light-harvesting, and gas binding.[6–11] The central metal ion significantly influences the electronic properties within the porphyrin ring.[12,13] Different metal ions exhibit distinct binding behaviors; for instance, nickel, zinc, and copper porphyrins tend to bind irreversibly to dioxygen,[14] whereas iron porphyrins efficiently bind oxygen but can oxidize in aqueous solutions without a protective protein environment, making oxygen binding irreversible.[15] The protein environment makes the water-mediated autoxidation less favorable, and the distal histidine residue reduces the affinity for other ligands such as carbon monoxide.[16]

Axial ligands also play a crucial role, affecting the electronic distribution and oxygen affinity of porphyrin systems.[17] In iron porphyrins with nitrogen-containing axial ligands, increased electron density around the nitrogen atom coordinated to the iron atom leads to higher binding energy and shorter Fe—O bond distance when binding dioxygen.[6] Axial ligands induce conformational changes in hemoglobin upon oxygen binding,[14] and their nature impacts the ability of the porphyrin to interact with other ligands or small molecules.[18] Substituents on the porphyrin ring further influence electronic properties, geometry, and interactions with ligands.[9,10]

In addition to conformational changes, ligands can also modify the spin state of the metal center. Imidazole-coordinated Co(II) porphyrins exhibit a low-spin ground state,[19] whereas Fe(II) porphyrins with imidazole axial ligands exhibit a high-spin.[20] Iron poprhyrins with an imidazole axial ligand exhibit different electronic structures than Fe(II) porphyrins coordinated to other ligands.[21] A key to understand the differences in electronic configuration of iron porphyrins with imidazole ligands is to determine which of the 3d orbitals is doubly occupied.[21] High-spin Fe(II) porphyrins with an imidazole ligand have been observed to have a $3d^6$ configuration with a doubly-occupied $3d_{xz}$ orbital.[21] Experimental work on deoxy-heme from sperm whales with a histidine axial ligand showed an equilibrium between two structures: one with the double occupancy on the $3d_{xy}$ orbitals and another with a doubly-occupied $3d_{xz}$ orbital, with the latter being the dominant structure.[22] Conversely, DFT calculations on iron porphyrins with an NHC axial ligand show a $3d^2$ occupancy.[23]

Despite extensive research into the effects of the individual building blocks of the porphyrin system, the complex interactions governing the oxygen affinity of metalloporphyrins remains elusive. This study aims to compare the binding energies and electronic density distributions of porphyrins with different metal ions, ring substituents, and axial ligands using DFT. By understanding how these components interact, we aim to gain deeper insights into the customization of porphyrins for applications that require specific properties to be tuned, such as the development of photosensitizers and catalysts, with a specific focus on elucidating the role of each building block in oxygen affinity.

2 | COMPUTATIONAL DETAILS

The selected porphyrin models for DFT calculations involve permutations of different metals (M), ring-substituents (R) and axial ligands (L) on a porphyrin (Table 1). The low (LS), intermediate (IS), and high spins (HS) were calculated for each molecule to determine their ground state. The DFT calculations were performed using the Gaussian 16 software package.[24] The functional B97D[25] was used with the basis sets def2-TZVP for the metal, and def2-SVP for the other atoms,[26] as we previously found this combination of basis set and functional provides reliable results with porphyrins in terms of binding energy, geometry, as well as spin states.[27] The binding energies were calculated using the zero-point energy (ZPE) corrected energies of the ground states on the different molecules. The binding energy to dioxygen (ΔE_B) was calculated as the difference between the ZPE-corrected energies of the sum of the individual metalloporphyrin (E_{MRL}) and O_2 (E_{O_2}) and the oxy-complex (E_{MRL-O_2}) (Equation 1).

$$\Delta E_B = E_{MRL} + E_{O_2} - E_{MRL} - O_2. \quad (1)$$

A total of 14 porphyrins were studied, each one optimized in their LS, IS, and HS states. To analyze the changes that occur on the binding to the oxygen with the different substituents, metals, and axial ligands. A natural bond orbital (NBO) analysis was performed to obtain the natural atomic charges (NAC) and the natural electronic configurations. The changes in the geometry of the molecule are analyzed based on the distance between the metal and the axial ligand ($M-L_{axial}$), the displacement of the iron atom from the plane formed by the four nitrogen atoms on the pyridin groups (ΔM) (Figure 1), the average distance between the opposing nitrogens in the porphyrin ring (N_P–N_P). For the oxygen bonded porphyrins, the distance between the metal and the oxygen (M—O), the oxygen–oxygen bond distance (O—O) and the angle between the metal and the dioxygen adduct (M—O—O) were calculated.

To assess the deformations of the porphyrin plane in the different molecules, first, a plane was fitted using the four nitrogens at the core of the porphyrin ring through a least-squares method. Then, the root mean square error ($RMSE_{plane}$) of the distances between the porphyrin atoms and this plane was calculated. Only the atoms within a 4.5 Å radius on the porphyrin plane from the metal atom were considered in calculating the $RMSE_{plane}$. This approach allowed to quantify the deviation from a perfectly planar porphyrin (i.e., $RMSE_{plane} = 0$).

TABLE 1 Metals (M), ring substituents (R), and axial ligands (L) on the porphyrin used on this work.

Abbreviation	Group	Name
M	Fe	Iron
M	Co	Cobalt
R	OEP	Octaethyl porphyrin
R	TPP	Tetraphenyl porphyrin
R	P	Porphyrin (No substituents)
L	Cl	Chlorine
L	Im.	Imidazole
L	NHC	1,3-Dimethylimidazolium

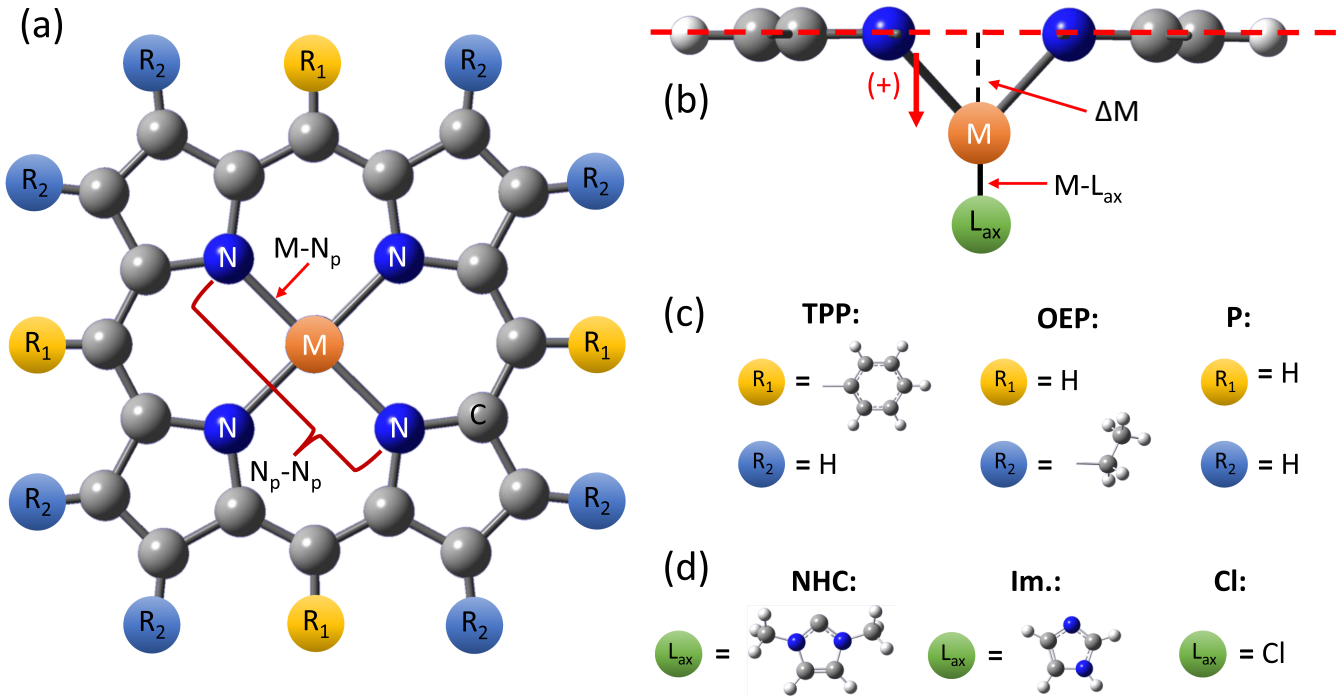

FIGURE 1 Porphyrin models used on this work. (A) Axial view of the porphyrin ring. (B) Lateral view of the porphyrin ring, showing the displacement of the metal atom with respect to the porphyrin plane (ΔM) and the distance from the metal to the axial ligand ($M–L_{axial}$). (C) Different substituents on the porphyrin ring. (D) Axial ligands.

3 | RESULTS AND DISCUSSION

3.1 | Ground states and relative energies

The ground state configurations of the studied molecules, including low-spin (LS), intermediate-spin (IS), and high-spin (HS) states, have been calculated and are presented in Table 2. For the cobalt deoxy-porphyrins, the ground state consistently corresponds to the low-spin state, regardless of the axial ligand or the presence of ring substituents.

In contrast, the ground state for iron porphyrins varies with the axial ligand. Chlorine and imidazole axial ligands lead to sextet and quintet ground states, respectively. On the other hand, iron porphyrins coordinated with NHC as an axial ligand exhibit a singlet, closed-shell ground state. Furthermore, experimental findings confirm the sextet ground state for iron porphyrins with a chlorine axial ligand.[28] Experimental studies on iron porphyrins with imidazole ligands have consistently reported a high-spin ground state[29] in agreement with our calculations.

The case of NHC as an axial ligand is distinctive, as it results in singlet ground state in iron porphyrins. This finding has been corroborated by experimental research on various carbenes coordinated to iron porphyrins,[30,31] as well as computational investigations involving different n-heterocyclic carbenes coordinated to phtalocyanines,[32] including the 1,3-dimethylimidazolium (NHC) ligand employed in this study. The LS ground state of the NHC-coordinated iron porphyrins is attributed to the more covalent nature of the C—Fe bond between the NHC and the metal cation observed in recent studies.[30,32] Interestingly, it has been observed that NHC with electron withdrawing substituents yields an IS ground state, and a much lower association energy with the metal porphyrin, compare to electron-donating NHCs.[32] Nonetheless, it is worth noting that the choice of the DFT method can impact the relative energies of different porphyrins, particularly when smaller basis sets are used, as observed in a recent study where FeTPPNHC was found to have a quintet ground state,[20] in contrast with the singlet ground state for the same molecule found in the literature and in this work.

Upon oxygen binding to the various porphyrins, some of them undergo spin state changes. This phenomenon has been widely documented in the literature, particularly for iron porphyrins coordinated to histidine, imidazole, and similar ligands.[5,33] In these cases, there is a spin crossover from the high-spin quintet state to an open-shell singlet state. Notably, this spin crossover was found in this work only for iron porphyrins coordinated to imidazole. Conversely, when NHC was employed as the axial ligand, the deoxy-porphyrins transitioned from a singlet to a triplet state.

In the case of cobalt porphyrins, they generally remain in a LS state upon binding oxygen, except for those coordinated to chlorine. Cobalt porphyrins with chlorine as an axial ligand undergo a transition from a HS to an IS state upon oxygen binding. Experimental data supports the tendency of cobalt porphyrins to remain in a low-spin state after binding oxygen with different axial ligands.[17,34]

These findings can explain the relatively high relative energies associated with the high-spin porphyrins coordinated to NHC and imidazole, which can be on the order of 20 kcal mol^{-1} for

TABLE 2 Relative energies of the different molecules analyzed in this work.

Molecule	LS	IS	HS
FeP	16.90	0.00	3.36
CoP	0.00	9.260	44.90
FePIm	3.44	0.46	0.00
CoPIm	0.00	11.03	43.80
FePCl	17.08	3.77	0.00
CoPCl	0.00	2.81	3.77
FePNHC	0.00	6.72	3.75
CoPNHC	0.00	9.13	39.31
FeOEPIm	3.41	0.41	0.00
CoOEPIm	0.00	11.27	36.95
FeOEPCl	17.29	3.65	0.00
CoOEPCl	0.00	2.21	3.52
FeOEPNHC	0.00	7.28	4.84
CoOEPNHC	0.00	9.68	32.93
FeTPPIm	3.51	0.21	0.00
CoTPPIm	0.00	11.08	41.41
FeTPPCl	16.28	3.60	0.00
CoTPPCl	0.00	3.01	4.51
FeTPPNHC	0.00	7.56	5.73
CoTPPNHC	0.00	10.74	38.93
FePIm-O_2	0.00	0.93	9.36
CoPIm-O_2	0.00	8.40	19.41
FePCl-O_2	0.00	9.90	0.71
CoPCl-O_2	10.43	0.00	4.12
FePNHC-O_2	5.75	0.00	15.16
CoPNHC-O_2	0.00	8.66	17.87
FeOEPIm-O_2	2.21	0.00	8.35
CoOEPIm-O_2	0.00	8.65	19.96
FeOEPCl-O_2	0.00	9.24	0.37
CoOEPCl-O_2	8.21	0.00	3.89
FeOEPNHC-O_2	7.37	0.00	14.97
FeTPPIm-O_2	2.19	0.00	8.24
CoTPPIm-O_2	0.00	8.42	20.04
FeTPPCl-O_2	0.00	9.76	0.32
CoTPPCl-O_2	5.40	0.00	5.44
FeTPPNHC-O_2	5.85	0.00	11.00
CoTPPNHC-O_2	0.00	10.65	20.24

Note: Energy differences given in kcal mol^{-1}.
Abbreviations: HS, high-spin; IS, intermediate-spin; LS, low-spin.

oxy-porphyrins. This difference is more pronounced in deoxy cobalt porphyrins, where the high-spin state can be up to 40 kcal mol^{-1} higher in energy than the low-spin ground state. These results illustrate the unfavorable nature of the high-spin state for cobalt porphyrins.

Overall, the spin state of the iron porphyrins seem to be solely defined by the nature of the axial ligand, while for cobalt porphyrins the spin state is determined by the metal and is relatively insensitive to the choice of axial ligand. The desired spin state of FeP could be obtained by choosing the ligand accordingly (or the ligand substituents), as it has been reported in the literature.[32]

3.2 | Effect of metal, ring substituents, and axial ligands on the binding energy

The binding energies of porphyrins with different ring substituents, axial groups, and metals are summarized in Figure 2. It is evident that the choice of an axial ligand plays a crucial role in determining a porphyrin's affinity for dioxygen, as previously suggested by DFT studies.[7,8] Generally, when the same axial ligand is used, the binding energies of porphyrins with various ring substituents differ by less than 3 kcal mol^{-1}. Cobalt porphyrins exhibit greater differences across different ring substituents, with maximum differences of 2.15, 2.12, and 1.04 kcal mol^{-1} for NHC, chlorine, and imidazole, respectively. Iron porphyrins show smaller differences with different axial ligands than cobalt porphyrins, with values of 1.33, 0.64, and 0.70 kcal mol^{-1} for NHC, Cl, and imidazole, respectively.

The use of imidazole as an axial ligand results in very similar binding energies regardless of the metal ion and ring substituent, with the greatest difference being 1.1 kcal mol^{-1} among all porphyrins with this axial ligand. Histidine, which contains an imidazole group, is the natural ligand in biological systems and provides the most reproducible affinities to O_2. In contrast, when NHC is used, differences between substituents and metals become more apparent, with maximum differences in the order of 6 kcal mol^{-1}. Cobalt porphyrins have, on average, binding energies 4.37 kcal mol^{-1} higher than iron porphyrins when NHC is the axial ligand. Among porphyrins coordinated to this ligand, those with phenyl substituents exhibit the highest binding energies, with 15.26 kcal mol^{-1} for CoTPPNHC and 10.69 kcal mol^{-1} for FeTPPNHC.

Similar disparities between metals are found when chlorine is used as an axial ligand. Cobalt porphyrins have average binding energies 5.1 kcal mol^{-1} higher than iron porphyrins with the same axial ligand. The TPP substituent results in higher energies than Cl-coordinated porphyrins with other substituents, with values of 7.34 kcal mol^{-1} for CoTPPCl and 1.4 kcal mol^{-1} for FeTPPCl. Notably, differences in binding energies across different ring substituents are smaller with Cl as an axial ligand compared to NHC. Among cobalt porphyrins, CoTPPCl exhibits a binding energy 2.12 kcal mol^{-1} higher than other cobalt porphyrins with this ligand. For iron, the difference in binding energy between FeTPPCl and its counterparts is only as high as 0.64 kcal mol^{-1}.

The calculated binding energies align with previous studies. Cobalt porphyrins had been reported to have binding energies in the range of 11–14 kcal mol^{-1},[14,35,36] while iron porphyrins and hemoproteins typically ranged from 13 to 19 kcal mol^{-1}.[15,37–39] Notably, the binding energies of cobalt porphyrins, which are usually lower than their iron counterparts and hemoproteins,[14,40] are significantly improved when NHC is used as an axial ligand, resulting in higher

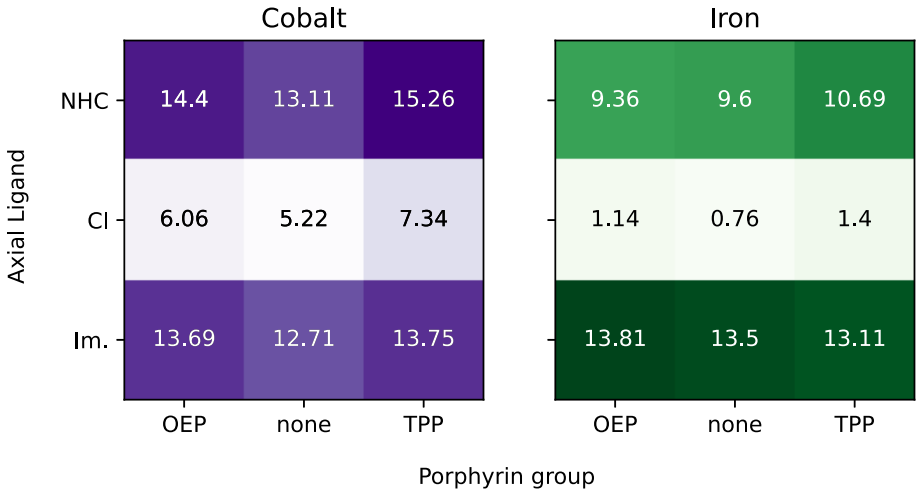

FIGURE 2 Binding energies of dioxygen to the different studied metalloporphyrins in kcal mol^{-1}. Vertical axis: axial ligands directly bonded to the metal ion. Horizontal axis: functional groups on the porphyrin ring. Purple: cobalt porphyrins. Green: iron porphyrins.

affinities than other iron porphyrins in this study. To the best of our knowledge, there are no experimental measurements or simulations of the affinity of NHC-coordinated cobalt porphyrins to O_2.

These results suggest that while the axial ligand directly coordinated to the active metal center significantly influences binding energies, the extent of this effect is moderated by the choice of metal cation. In other words, for most of the studied porphyrins, the axial ligand determines the order of magnitude of the interaction, while the metal cation (and the ring substituent) defines the precise energy within the interaction governed by the axial ligand. Notwithstanding, when imidazole is employed, the effects of the metal ion and ring substituents on the interaction with O_2 seem to be obscured by the effect of this axial ligand. Overall, the results presented in this work demonstrate that the affinity of metalloporphyrins to O_2 can be modulated in discrete steps in the order of 1 kcal mol^{-1} and in the range of 1–15 kcal mol^{-1}.

3.3 | Geometries of deoxy-porphyrins

The bond distances between the metal center and the axial ligand ($M–L_{axial}$) show little dependency on the ring substituents, as presented in Figure 3A. The shortest distances overall were found when NHC and imidazole are used, and they are longer with chlorine as an axial ligand, with the shortest distances corresponding to the iron porphyrins with the NHC axial ligand. For the cobalt porphyrins, the $M–L_{axial}$ bond distances to NHC and imidazole are all in the order of 2.1 Å. Conversely, when iron is used, the $M–L_{axial}$ of the porphyrins containing NHC is shorter and in the order of 1.9 Å. The difference between NHC and imidazole is more evident for iron porphyrins, albeit both NHC and imidazole distances being shorter than those of the chlorine-containing porphyrins. In summary, NHC and imidazole result in shorter $M–L_{axial}$ bond distances, but with iron, the NHC axial ligand results in a tighter bond compared to imidazole and chlorine. The explanation for the tighter bond between NHC and Fe can be ascribed to the unusual spin state of iron porphyrins coordinated to carbenes. Experimental data has shown that carbene-coordinated iron porphyrins and phtalocyanines are diamagnetic and predominantly in a low-spin (LS) state,[30–32] which is also observed in this work for NHC, whereas when imidazole or chlorine is used, the ground state of the iron porphyrins is high-spin (HS).

The calculated displacement of the metal atom from the porphyrin plane (ΔM) for deoxy-porphyrins is presented in Figure 3B.

The imidazole ligand displaces the least the cobalt atom compared to iron. The porphyrins containing NHC resulted in similar displacements irrespective of the ring substituents, and both iron and cobalt porphyrins lie in the range of 0.17–0.22 Å. The iron porphyrins with imidazole as an axial ligand exhibit slightly longer ΔM than the NHC-coordinated porphyrins, in the order of 0.01–0.06 Å longer, but significantly longer than the cobalt porphyrins with imidazole, which exhibit displacements in the order of 0.133 Å shorter than the iron porphyrins with imidazole.

Overall, when NHC is used as an axial ligand, the displacements vary little with the different metals, and even less with the change of ring substituents. With imidazole, the displacement is greatly affected by the metal center. This could be explained by the finding that the studied porphyrins with NHC as an axial ligand consistently exhibit a low-spin ground state, whilst with imidazole the iron porphyrins have a HS ground state. This agrees with earlier reports on the literature, where Co(II) porphyrins have LS electron configurations, whereas the iron porphyrins are predominantly HS.[17,34] The differences in ΔM and $M\text{-}N_P$ distances are largely explained by these differences in ground states.[17]

These differences are also apparent when chlorine is used as an axial ligand. Cobalt porphyrins seem to yield LS configurations regardless of the ligands, whereas the iron porphyrins with this axial ligand have a sextet (HS) ground state. The iron porphyrins with a chlorine axial ligand also exhibited the lowest binding energies. It is reasonable to expect that a metal center that is further pulled toward the chlorine atom will have a smaller interaction with the oxygen on the opposite axial coordination site. With this exception, the binding energies do not seem to be strictly related with the displacement of the metal atom. This can be easily observed with the cobalt porphyrins with a chlorine axial ligand (Figure 3B, light green markers), whose binding

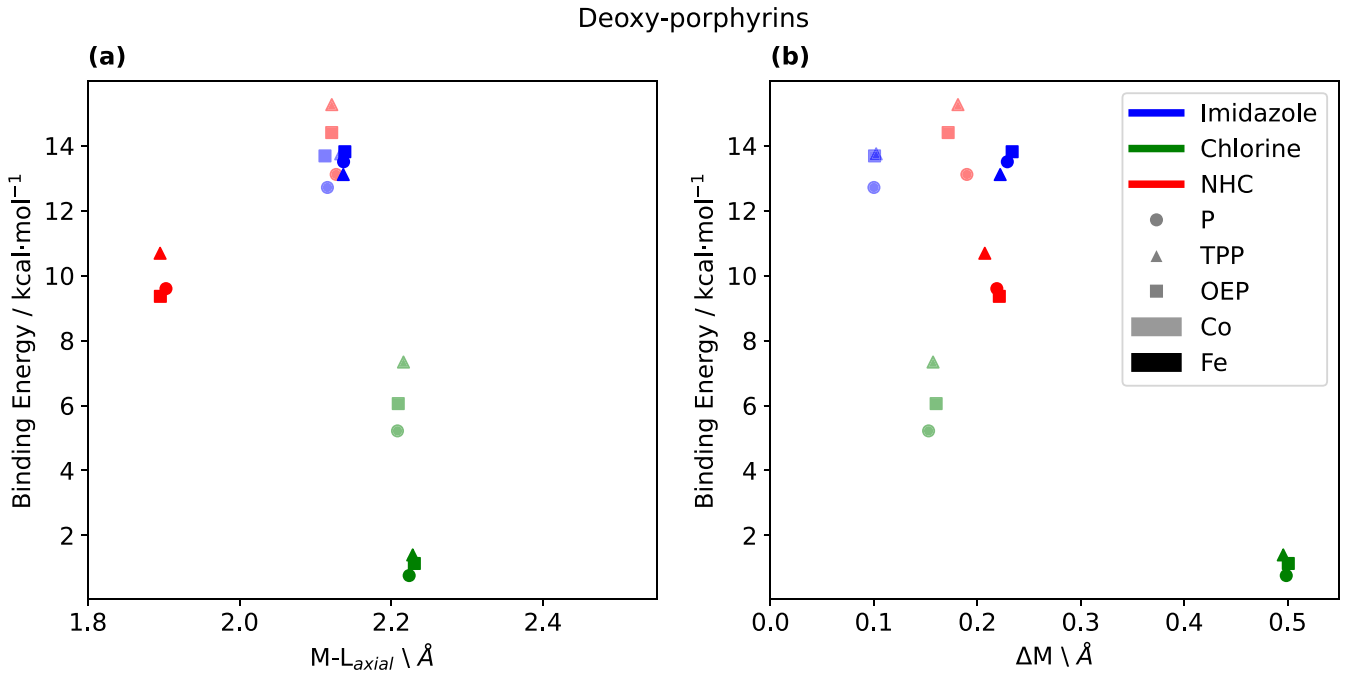

FIGURE 3 Geometrical parameter of deoxy-porphyrins (horizontal axis) and their resulting binding energy to O_2. (A): Distance between the metal center and the axial ligand (M–L_{axial}). (B) Displacement of the metal atom from the plane formed by the 4 pyrrole nitrogen atoms (ΔM). Marker color: axial ligand; marker shape: ring substituents; bold or light color: Iron or Cobalt as metal centers, respectively.

energies (5.22–7.34 kcal mol^{-1}) are as low as half of the binding energy of imidazole and NHC-coordinated porphyrins (9.6–15.2 kcal mol^{-1}) albeit exhibiting similar displacements of the metal (0.153–0.160 Å).

The average N_P–N_P distances provide some insight on the opening of the porphyrin ring center (Figure 4). For the cobalt porphyrins, the N_P–N_P distances were the largest with the imidazole ligand, closely followed by chlorine. The shortest N_P–N_P distances were obtained with NHC as an axial ligand. It is noteworthy that the differences in N_P–N_P distances are smaller than.

0.082 Å, and in some cases they can be as small as 0.02 Å. In the case of the iron porphyrins, the imidazole resulted in larger N_P–N_P distances, followed by chlorine. The NHC ligand resulted in the smallest distances. In contrast, the iron porphyrins with an imidazole ligand resulted in significantly larger N_P–N_P distances compared to the cobalt porphyrins coordinated to imidazole and chlorine. The N_P–N_P distances in iron porphyrins can be up to 0.139 Å larger than those in cobalt porphyrins when imidazole is used, and up to 0.117 Å larger with the chlorine axial ligand. Conversely, when the porphyrins were coordinated to NHC, the N_P–N_P distances were comparable between cobalt and iron porphyrins, with differences in the order of 0.014–0.036 Å between them.

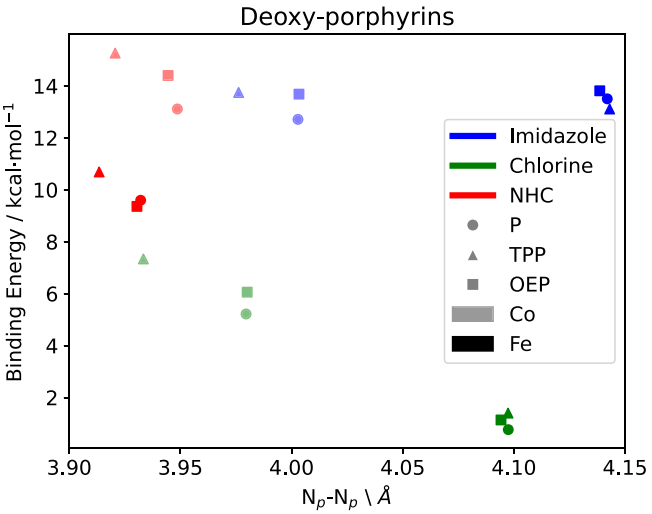

FIGURE 4 Average N_P–N_P distances for the different deoxy-porphyrins (horizontal axis) and their resulting binding energy to O_2. Marker color: Axial ligand; marker shape: Ring substituents; bold or light color: Iron or Cobalt as metal centers, respectively.

3.4 | Geometries of oxy-porphyrins

In terms of M–L_{axial} bond distances, as presented in Figure 5A, the oxygenated porphyrins generally exhibit longer bond lengths when chlorine is used as a ligand, in comparison to imidazole and NHC. Notably, when NHC or imidazole serve as an axial ligand, the M–L_{axial} distances are within a 0.1 Å range of each other. Specifically, the cobalt porphyrins demonstrate a remarkable agreement (within 0.01 Å) when coordinated with NHC and imidazole. However, in the case of chlorine, the differences extend to around 0.08 Å. For iron porphyrins, using Cl as an axial ligand also results in the longest distances, followed by imidazole, and with NHC yielding the shortest

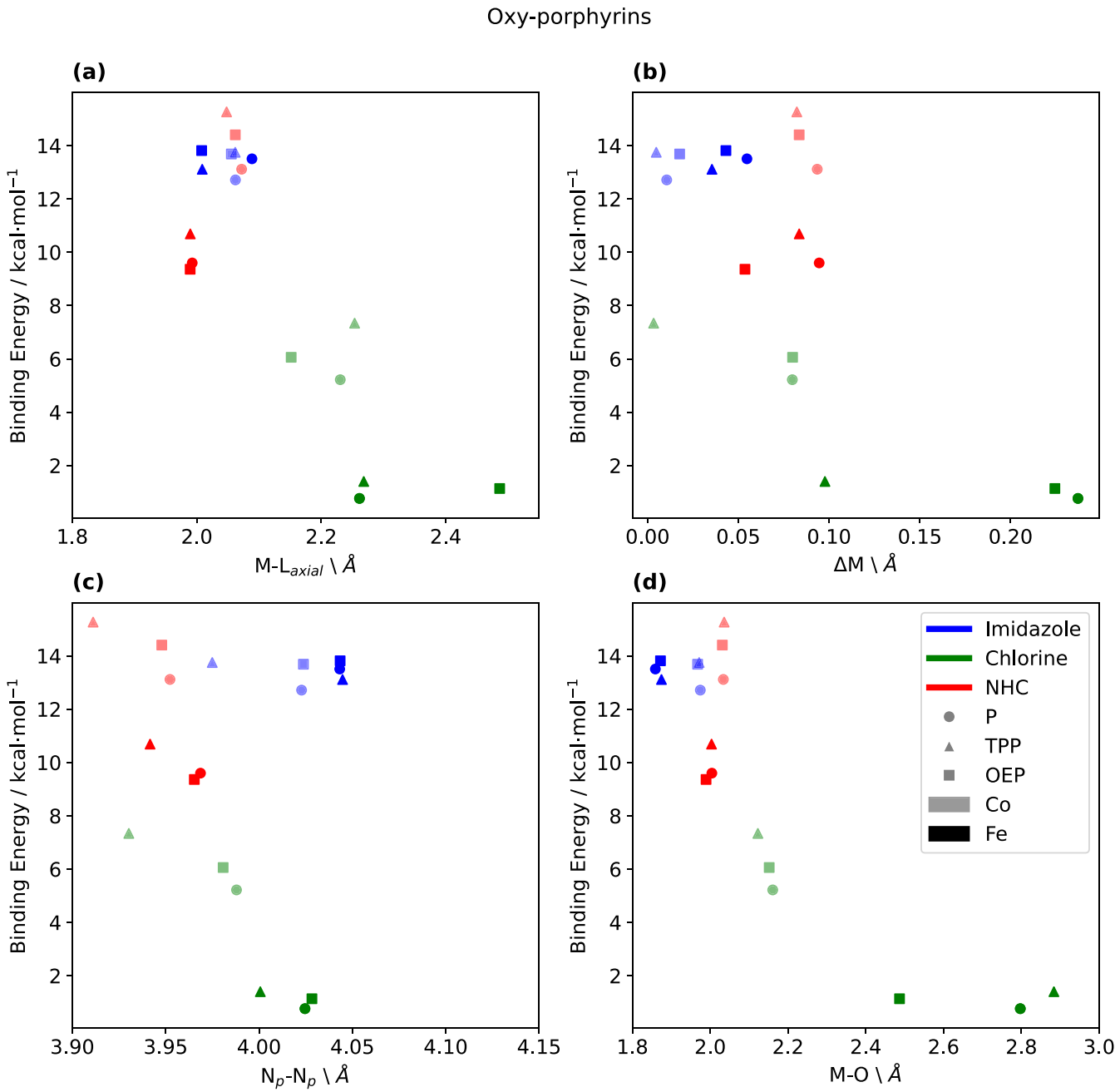

FIGURE 5 Geometrical parameters of oxy-porphyrins (horizontal axis) and their resulting binding energy to O_2. (A) Distance between the metal center and the axial ligand (M–L_{axial}). (B) Displacement of the metal atom from the plane formed by the 4 pyrrole nitrogen atoms (ΔM). (C) Average distance between opposing pyrrole nitrogen atoms (N_P–N_P). (D) Bond distance between the metal cation and the proximal oxygen atom (M–O). Marker color: axial ligand; marker shape: ring substituents; bold or light color: iron or cobalt as metal centers, respectively.

M–L_{axial} lengths. It is interesting to note that the unsubstituted FeP with an imidazole ligand also exhibits longer M–L_{axial} lengths when compared to FeTTPIm and FeOEPIm. This trend, observed in cobalt porphyrins and imidazole-coordinated iron porphyrins, is not present with Cl and NHC. Given the variations in the degree of deformation from planarity among the porphyrins, these differences in M–L_{axial} lengths between cobalt and iron porphyrins may also be attributed to these deformations of the porphyrin plane, a topic which will be discussed in Section 3.5.

In the displacement of the metal atoms (ΔM), consistent trends emerge among the studied porphyrins, as illustrated in Figure 5B. In both cobalt and iron porphyrins, the use of an imidazole ligand results in the smallest ΔM values, falling within the range of 0.001–0.002 Å for cobalt and 0.007–0.011 Å for imidazole-coordinated iron porphyrins. These findings suggest that when imidazole is used as the axial ligand, the metal atom is significantly drawn back into the porphyrin plane upon binding to O_2. In contrast, NHC-coordinated porphyrins exhibit larger ΔM displacements compared to those with imidazole as

the axial ligand, while also being pulled into the porphyrin plane following O_2 binding. Nevertheless, porphyrins with NHC as the axial ligand show very similar displacements, regardless of the metal or the ring substituents. This is consistent with the displacements of deoxy-porphyrins (Figure 3B), where the use of NHC resulted in minimal differences in ΔM between metals and different ring substituents, while their variations in binding energies ultimately depended on the metal center. In contrast, when imidazole is used, the larger differences observed in deoxy-porphyrins are significantly reduced upon O_2 binding.

For cobalt porphyrins with a Cl axial ligand, ΔM values are closer to those of NHC- and imidazole-coordinated porphyrins, rather than with the ΔM of iron porphyrins also coordinated to chlorine. While NHC-coordinated porphyrins for both metals exhibit differences in ΔM in the order of 0.001 Å, the differences between cobalt and iron porphyrins with chlorine as an axial ligand are in the order of 0.05 Å, with iron porphyrins displaying the greatest ΔM values. A difference between Co and Fe porphyrins can be deduced: NHC results in the largest ΔM for cobalt porphyrins, while for iron, significantly larger differences are observed with chlorine. Surprisingly, despite the differences in size between Cl and NHC, including their widely different steric effects, the displacement of the iron atom with NHC is over half of that obtained with Cl.

Notably, despite the small binding energy and the longer M—O distances obtained with iron porphyrins when chlorine is used as an axial ligand, suggesting a relatively weak interaction with O_2, the iron atom is notably pulled toward the porphyrin plane after binding O_2.

The calculated N_P–N_P distances, presented in Figure 5C, reveal a consistent pattern across most of the porphyrins. With the exception of imidazole-coordinated porphyrins, the N_P–N_P distances show a consistent pattern of decreasing binding energy with the increasing N_P–N_P distance. The tetraphenyl-substituted porphyrins, denoted by triangle markers in Figure 5C, exhibit shorter N_P–N_P distances compared to the octaethyl and unsubstituted porphyrins. The iron porphyrins with imidazole are an exception, as they exhibit very similar N_P–N_P distances, regardless of the ring substituent. Among the cobalt porphyrins with NHC as an axial ligand, CoTPPNHC, with its tetraphenyl substituents, has a N_P–N_P distance that is 0.04 Å shorter than the other porphyrins. When imidazole is used as the axial ligand in cobalt porphyrins, the N_P–N_P distance of CoTPPIm is 0.05 Å shorter than its counterparts. The largest difference is observed in the case of CoTTPCl, which has a N_P–N_P distance 0.06 Å shorter than the other cobalt porphyrins with chlorine as an axial ligand. The NHC-coordinated iron porphyrins exhibit a similar trend, with FeTPPNHC displaying N_P–N_P distances that are 0.05 Å shorter than those of OEP and unsubstituted porphyrins. In contrast, the iron porphyrins coordinated with imidazole, such as FeTPPIm, have N_P–N_P distances only 0.002 Å longer than their counterparts. The results of the N_P–N_P distances reveal that imidazole yields the greatest distances, followed by chlorine, with NHC resulting in the shortest distances. Although the differences are small, the same trend is observed for both metals.

The bond distances between the metal atom and the proximal oxygen (M—O) are presented in Figure 5D. The porphyrins coordinated with imidazole exhibit the shortest bond lengths, with the iron porphyrins having the shortest M—O distances overall. When cobalt porphyrins have imidazole as an axial ligand, their M—O distances are approximately 0.1 Å longer than those of iron porphyrins with the same axial ligand. However, for all the porphyrins coordinated to NHC, the M—O distances are consistently within a narrow range, varying by only 0.047 Å regardless of the metal or the ring substituent.

In contrast, when chlorine is used as an axial ligand, cobalt porphyrins have M—O distances that are 0.127 Å longer compared to when NHC is used, and 0.186 Å longer than cobalt porphyrins coordinated with imidazole. The changes in M—O distances are more pronounced for the iron porphyrins. For instance, the M—O lengths of FeTPPCl-O_2 are 1 Å longer than those calculated for FeTPPIm-O_2, and 0.841 Å longer than those of FeTPPIm-O_2. Furthermore, the differences in M—O distances between the various ring substituents are more evident in the chlorine-coordinated porphyrins, with the largest difference being 0.357 Å between FeTPPCl-O_2 and FeOEPCl-O_2.

It is noteworthy that although the highest binding energies are generally obtained with the smaller M—O distances among the studied porphyrins, the porphyrins with the highest binding energies, such as Cobalt porphyrins with NHC, do not exhibit the shortest M—O bond lengths (Figure 5D, light red markers). In fact, the iron porphyrins coordinated with imidazole display comparable binding energies to those of NHC-coordinated cobalt porphyrins, yet their M—O distances are approximately 0.12–0.15 Å shorter. Similarly, the iron porphyrins with NHC as the axial ligand yield M—O bond lengths similar to those of cobalt porphyrins with NHC, while having binding energies 4.4 kcal mol^{-1} lower.

The angles between the metal center and the dioxygen adduct (M—O—O) are presented in Figure 6A. Among these, the iron porphyrins coordinated with chlorine as an axial ligand exhibit the shortest angles, measuring approximately 121.4–122.1°. In contrast, cobalt porphyrins with a chlorine ligand tend to have larger angles compared to chlorine-coordinated porphyrins and other cobalt porphyrins. When cobalt porphyrins have imidazole and NHC as axial ligands, their angles are similar, differing by only around 1.361°. Notably, the iron porphyrins coordinated to NHC display the largest M—O—O angles, typically around 131°.

The O—O bond distances of the O_2 adducts are depicted in Figure 6B. The cobalt porphyrins with an NHC ligand exhibit some of the longest bond distances, followed by the imidazole-coordinated porphyrins, irrespective of the metal. Interestingly, the O—O distances for the porphyrins with an imidazole axial ligand are somewhat consistent, differing by only about 0.01 Å from one another. This is in stark contrast to the differences observed between NHC and Cl-coordinated porphyrins, where the maximum variations are on the order of 0.023 and 0.020 Å, respectively. It appears that the nature of the axial ligand does not entirely determine the resulting O—O bond distances in the dioxygen ligand. NHC-coordinated porphyrins, however, do exhibit variations in the stretching of the O—O bond depending on the metal center, with cobalt porphyrins having the longest O—O distances. This same pattern is present when Cl is the axial

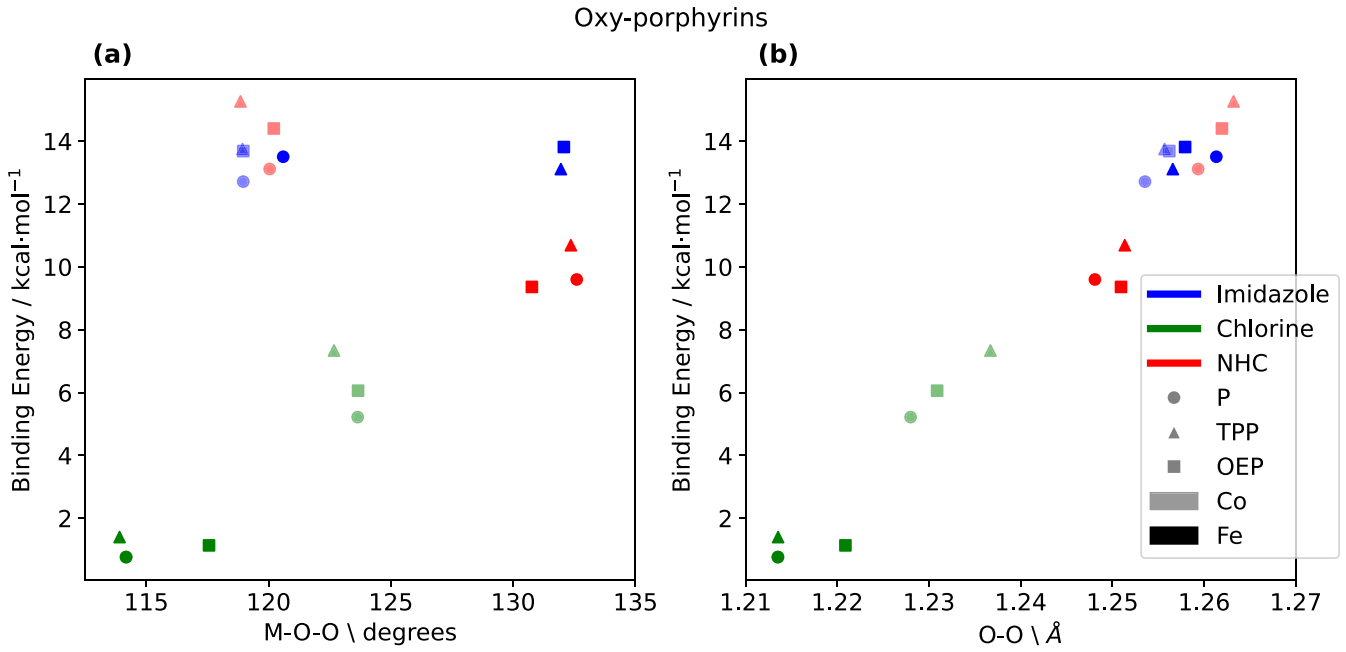

FIGURE 6 Geometrical parameters of oxy-porphyrins (horizontal axis) and their resulting binding energy to O_2. (A) Bond angle between the metal cation and the O_2 adduct (M–O–O). (B) Bond distance between the oxygen atoms in the O_2 adduct (O–O). Marker color: axial ligand; marker shape: ring substituents; bold or light color: iron or cobalt as metal centers, respectively.

ligand: cobalt porphyrins have larger O—O bonds compared to iron porphyrins.

In the context of O_2 binding to metalloporphyrins, previous research has identified a correlation between stronger binding energies and the weakening (and subsequent lengthening) of the O—O double bond, as well as a clear association between increased binding energy and reduced M—O bond lengths.[41] However, in the present work, while we observed a correlation between higher binding energies and longer O—O bonds, the M—O bond lengths did not consistently follow this trend. Other computational studies have also found where greater binding energies leading to shorter M—O distances.[6] Specifically, iron porphyrins with an imidazole ligand (Figure 5D, bold blue markers) exhibited the shortest M—O lengths. In contrast, other porphyrin complexes, such as those featuring cobalt coordinated to NHC (Figure 5D, light red markers), displayed comparable or even higher binding energies while simultaneously featuring longer M—O bonds.

The O—O distances in porphyrins with an imidazole ligand were slightly shorter than those in cobalt porphyrins coordinated to NHC (Figure 6B). These findings suggest that while these correlations are useful heuristics, the exact distances are influenced by the specific combination of metal, axial ligand, and, to a lesser extent, the ring substituent.

To illustrate this, let us consider CoTPPNHC and FeTPPIm after oxygenation. CoTPPNHC-O_2 exhibits a M—O distance of 2.036 Å, an O—O distance of 1.263 Å, and a binding energy of 15.26 kcal mol^{-1}. In contrast, FeTPPIm-O_2 features a M—O distance of 1.875 Å, an O—O distance of 1.267 Å, and a binding energy of 13.11 kcal mol^{-1}. Despite CoTPPNHC-O_2 having a longer M—O bond and a comparable, albeit shorter, O—O bond, it exhibits a binding energy 2.15 kcal mol^{-1} higher than FeTPPIm- O_2. Iron porphyrins with a SH axial ligand have been reported to follow similar trends, where the M—O distance was 1.940 Å, the O—O distance 1.356 Å, and the binding energy 17.87 kcal mol^{-1}, in contrast to the same iron porphyrin with a 2-methylimidazole, which featured a M—O length of 1.891 Å, an O—O length of 1.345 Å, and a binding energy of 8.69 kcal mol^{-1}.[6] These observations suggest that, in our work and in the literature, the O—O distance consistently corresponds to the magnitude of the binding energy, whereas the M—O bond distance appears to be reliant on the specific combination of metal and axial ligand.[6,41] It seems that when imidazole is used as an axial ligand, the effects of the metal and the ring substituents on some of the geometrical parameters are less evident. With NHC, there is a clear difference in the geometrical parameters between cobalt and iron porphyrins, but less on the ring substituent. It is also important to mention that when imidazole is used, the binding energies also lie within close range, despite the different substituents or metals, which is clearly not the case with NHC, let alone Cl. A clear trend involving the binding energy is observed for all the studied systems. The larger the binding energy of the porphyrin to O_2, the larger the O—O bond lengths calculated for the dioxygen adduct.

3.5 | Planarity and deformations of the porphyrins

The deformations of the porphyrin plane, as depicted in Figure 7, appear to vary significantly based on the choice of axial ligand and ring substituents. The NHC axial ligand leads to the most substantial

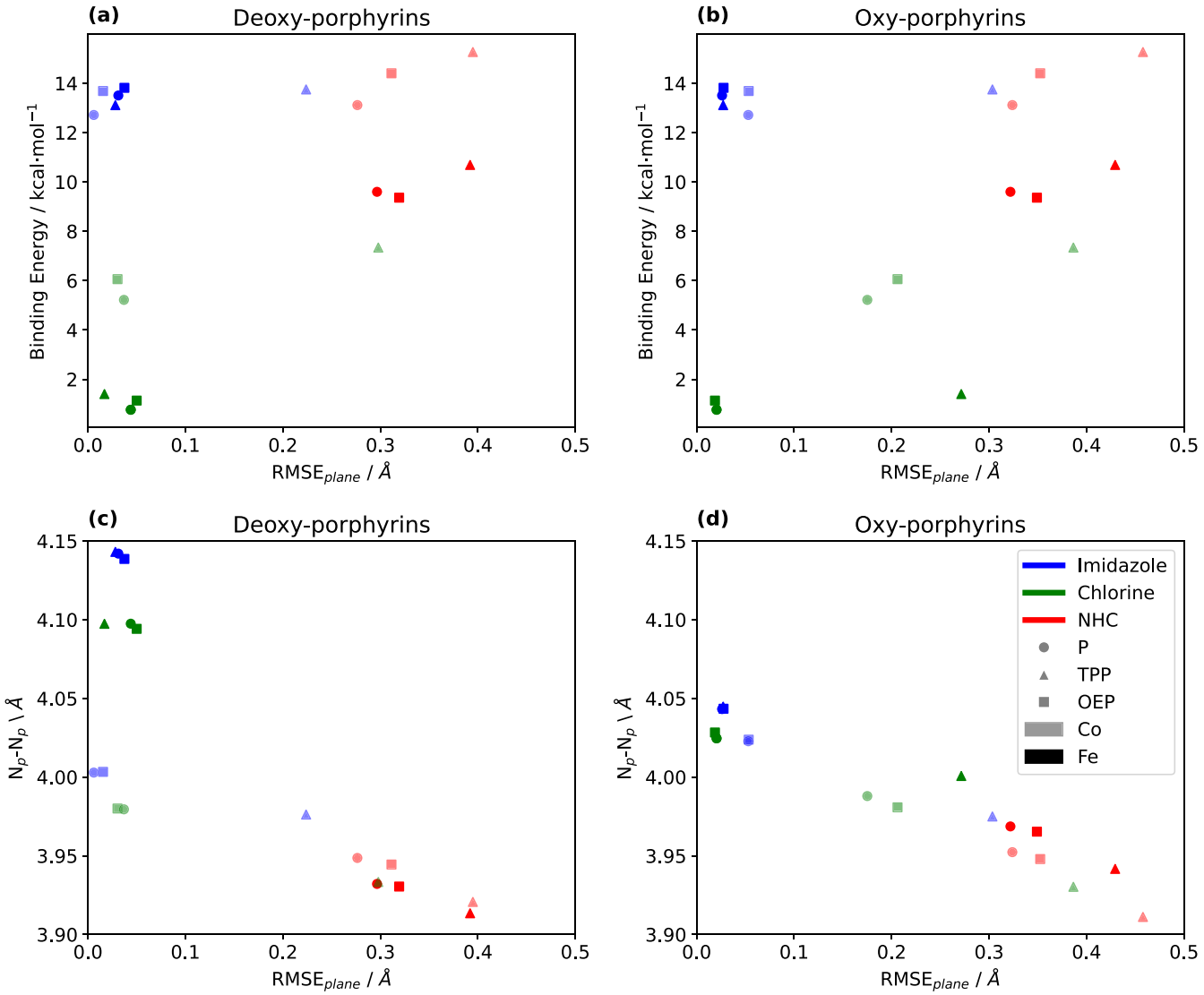

FIGURE 7 (A,B): Planarity of the porphyrin ring ($RMSE_{plane}$) before (A) and after (B) oxygen binding and the resulting binding energy. (C,D): $RMSE_{plane}$ (horizontal axis) and size of the porphyrin core measured as the average N_P–N_P distances before (C) and after oxygen binding (D) (vertical axis). Marker color: axial ligand; marker shape: ring substituents; bold or light color: iron or cobalt as metal centers, respectively.

deformations of the porphyrin plane (Figure 7, red markers). In contrast, when imidazole is used, the deformations are notably smaller (Figure 7, blue markers), with a noteworthy exception: CoTPPIm-O_2 exhibits a deformation more closely resembling those obtained with NHC (Figure 7B, light blue triangle). This structural stability induced by imidazole could be one of the reasons why natural selection chose the imidazole-containing amino-acid histidine to serve as the axial ligand of the heme group in hemoglobin.

It is worth noting that iron porphyrins coordinated to imidazole maintain significant planarity, regardless of the ring substituents. It appears that, for iron porphyrins, planarity is primarily determined by the axial ligand. When NHC or chlorine is employed instead, the tetraphenyl porphyrins consistently display greater deformations, followed by the octaethyl- and unsubstituted porphyrins.

In cases where chlorine is the axial ligand, the phenyl substituents seem to induce more pronounced changes in planarity compared to porphyrins featuring other axial ligands. Additionally, with NHC as the axial ligand, the unsubstituted and octaethyl porphyrins exhibit similar deformations, regardless of the metal. However, for tetraphenyl porphyrins, cobalt leads to greater deformations.

Notably, CoTPPNHC displays both the highest binding energy and deformation among all the studied porphyrins. It is possible that despite being significantly distorted into a saddled geometry, this shape contributes to the thermodynamic favorability of O_2 binding.

The shifts in planarity upon O_2 binding, as depicted in Figure 7A,B, highlight the distinct planar nature of iron porphyrins coordinated with imidazole. Within this group, O_2 binding leads to a decrease in $RMSE_{plane}$, indicating a trend toward increased planarity in the porphyrin ring after oxygen binding (Figure 7B, bold blue markers). In contrast, for most of the other porphyrins, O_2 binding induces an increase in the $RMSE_{plane}$, signifying that the oxygen adduct prompts additional distortions. Notably, cobalt porphyrins with imidazole or

NHC axial ligands exhibit similar changes in planarity across different ring substituents, unlike iron porphyrins, which display larger changes on the $RMSE_{plane}$ values after O_2 binding with NHC compared to imidazole. These differences could be partially explained by the ground states of the different porphyrins before and after oxygen binding. While cobalt porphyrins with NHC and imidazole remain in a LS state after O_2 binding, iron porphyrins with imidazole move from a HS to LS, whereas those with NHC as an axial ligand change from LS to IS (Table 2).

Conversely, porphyrins with Cl as an axial ligand exhibit significantly distinct changes depending on the metal used. Notably, FeTPPCl exhibits the most substantial alteration in planarity following O_2 binding.

Some studies pointed out that the shorter the M–N_p distances, and the smaller the porphyrin core (N_P–N_P) the more ruffled the porphyrin plane is observed.[42,43] By plotting the porphyrin core size (N_P–N_P) as function of the $RMSE_{plane}$, it can be observed that for the studied porphyrins this trend is also observed for oxy-porphyrins (Figure 7D). Likewise, a more deformed porphyrin plane also inversely correlates to the M–N_P distances, but not to the displacement of the metal atom. It seems that ΔM is preeminently determined by the interactions with the axial ligands, irrespective of the deformations of the porphyrin plane or the widening of the porphyrin core.

Earlier reports have pointed out that larger metal centers tends to yield more planar conformations than smaller metals, and that non-planar porphyrins tend to have smaller porphyrin cores.[44] Specifically, Fe(II) has an ionic radius of 0.74 Å, while Co(II) has an ionic radius of 0.65 Å.[45] This observation aligns with the trends observed in deformation for the various oxy- porphyrins on this work. In Figure 7D, it can be seen that although cobalt porphyrins result in smaller porphyrin cores compared to their iron counterparts, the relationship between core size and distortion is strongly influenced by the choice of axial ligand on the metal center. Notably, the differences in planarity between iron and cobalt porphyrins are less pronounced when NHC or imidazole is used as the axial ligand. When NHC is employed, a clear distinction emerges between the various porphyrin ring substituents in terms of their $RMSE_{plane}$ values (MPNHC < MOEPNHC < MTPPNHC; M = Fe, Co). However, when imidazole is the axial ligand, all substituents tend to cluster around similar core sizes and planarity, except for CoTPPIm-O_2, which exhibits deformations closer to those of NHC-coordinated porphyrins. Overall, while smaller metal centers tend to yield smaller porphyrin cores and greater plane deformations, the resulting degree of plane deformation is further influenced by the porphyrin substituents, with the phenyl groups inducing the greatest deformations. Ultimately, the resulting planarity is a combination of the effects of both the cation and substituents.

However, these trends do not apply in the same way to deoxy-porphyrins (Figure 7C). For iron porphyrins, larger cores compared to cobalt porphyrins are only observed when imidazole and chlorine are used as axial ligands. Surprisingly, cobalt porphyrins with these axial ligands exhibit similar or even more planar porphyrin rings than their iron counterparts. Similar to the observations with oxy-porphyrins, the cobalt porphyrins with tetraphenyl substituents deviate significantly, showing greater distortion compared to other imidazole- and chlorine-coordinated porphyrins. On the other hand, porphyrins with NHC as an axial ligand exhibit significantly greater distortions than other porphyrins. Interestingly, cobalt porphyrins exhibit slightly larger cores than iron porphyrins, contrary to the reports from literature[44] and the trends observed in the oxy-porphyrins in our study.

In summary, the planarity of the studied porphyrins appears to be influenced by both the axial ligand and the porphyrin substituents. For most of them, the presence of the phenyl substituents induces greater distortions, even with small axial ligands as chlorine. Notably, the planarity of porphyrins containing imidazole does not seem to be significantly affected by the ring substituent. To explore further these differences the natural charges, electronic configurations, and orbital occupancies of the metal 3d orbitals will be analyzed.

3.6 | Natural atomic charges and electronic configurations

The changes on the calculated natural atomic charges (NAC) on the metal atoms are presented in Figure 8. The most drastic changes in the charge are those of the iron porphyrins with an imidazole axial ligand (Figure 8, bold blue markers). The charges of the iron atom decrease by −0.755, −0.831, and −0.839 after O_2 binding for FePIm, FeOEPIm, and FeTPPIm, respectively. The Iron porphyrins with chlorine as an axial ligand (Figure 8, bold green markers) have the second largest increase in their charge, with −0.439, −0.493, and −0.431 for FePCl, FeOEPCl, and FeTPPCl.

On the other hand, the changes on charge for cobalt porphyrins and the iron porphyrins with NHC as an axial ligand are smaller and in the order of −0.2. In the case of cobalt porphyrins, the changes for the NHC and imidazole-coordinated porphyrins (Figure 8, light blue

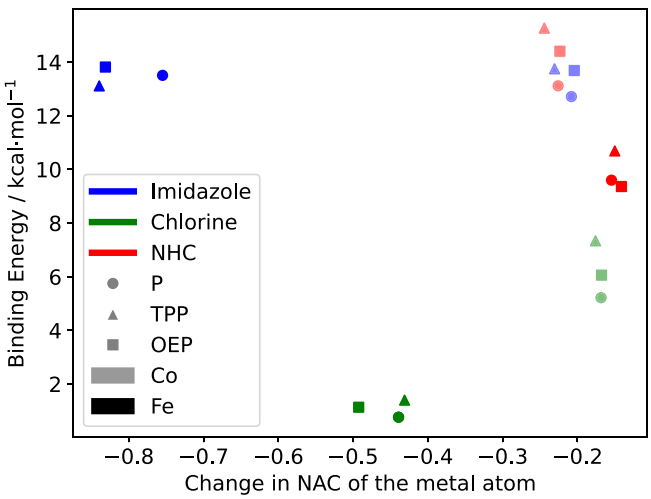

FIGURE 8 Change on the natural atomic charges (NAC) on the metal atoms after O_2 binding (horizontal axis) and their resulting binding energy to O_2. Marker color: axial ligand; marker shape: ring substituents; bold or light color: iron or cobalt as metal centers, respectively.

and red markers) are in close proximity to one another, all six systems lying between changes of −0.244 and −0.204. The iron porphyrins with NHC as an axial ligand exhibit the smallest change in charge, with −0.155, −0.141, and −0.150 for FePNHC, FeOEPNHC and FeTPPNHC, respectively (Figure 8, bold red markers).

The NAC on the oxygen atoms of the porphyrin-O_2 adduct are presented in Figure 9A for the proximal oxygen (O_a) and in Figure 9B for the distal oxygen atom (O_b). In the case of the proximal oxygen, the lowest charges were calculated for the cobalt porphyrins with NHC and imidazole as axial ligands (Figure 9A, light red and blue markers). Although small, the NHC-coordinated cobalt porphyrins have the largest negative charge on the cobalt atom, with −0.063, −0.067, and −0.073 for CoPNHC-O_2, CoOEPNHC-O_2, and CoTPPNHC-O_2. These are followed by the cobalt porphyrins with imidazole as an axial ligand, in the order of −0.039. The charges on O_a of the remaining porphyrins seem to be very close to neutral ranging between −0.003 and 0.008.

The NAC on the distal oxygen show a more clear pattern (Figure 9B). The higher the binding energies, the more negative the charge on O_b. The lowest charges were calculated for the cobalt porphyrins with NHC as an axial ligand, followed by the porphyrins coordinated with imidazole, and then the iron porphyrins with NHC. A similar trend, observed on many geometrical parameters and binding energies is also present here: when the axial ligand is imidazole, the differences between the two metal centers seem to be smaller, than those differences with NHC or Cl. The iron porphyrins with chlorine as axial ligand were calculated to have charges close to neutral for O_a and O_b, meaning that the charge distribution around O_2 is close to that of free-dioxygen. This is consistent with the shortest O—O bonds, longer M—O bonds, and small binding energies calculated for iron porphyrins with chlorine. The NAC shed some light on the differences between the different porphyrins. The electronic behavior of the different porphyrins can be further understood by analyzing the occupancies of the 3d orbitals of their metal centers.

The occupancy of the $3d_x2–y2$ orbital of the metal atoms in the different porphyrins is presented in Figure 10A for the deoxy- porphyrins and in Figure 10B after O_2 binding. The tetraphenyl cobalt porphyrins all showed a $3d_x2–y2$ occupancies closer to 1, compared to the almost doubly-occupied $3d_x2–y2$ orbitals on octaethyl and unsubstituted porphyrins (Figure 10A, light triangle markers). With the iron porphyrins, this was also observed when NHC was used as an axial ligand, but not when chlorine or imidazole were used, as in these two cases the $3d_x2–y2$ were singly occupied. Figure 11 presents the N_P–N_P distances as a function of the occupancy of the $3d_x2–y2$ orbital of the metal atom. The differences in this geometric parameter for the tetraphenyl porphyrins are consistent with the lower occupancies of the $3d_x2–y2$ orbital. For each metal and axial ligand (except imidazole) all the TPP molecules had shorter N_P–N_P distances compared to their counterparts with the same metal and axial ligand. These TPP also exhibit the occupancies closer to 1 before oxygen binding. Interestingly, the iron porphyrins containing imidazole do not show such trends.

After O_2 binding, the distinctions between the tetraphenyl-substituted porphyrins and the others become more pronounced, with one notable exception being when imidazole is used as an axial ligand. Across all tetraphenyl porphyrins (TPP), regardless of the metal or axial ligand, their $3d_x2–y2$ orbital remains close to be singly occupied. In contrast, most of their counterparts exhibit occupancies much closer to double occupancy of the same orbital upon O_2 binding. The FeTPPIm is the only TPP whose $3d_x2–y2$ occupancy increases after binding O_2. in stark contrast, the CoOEPIm is the only porphyrin that lowered the occupancy of this orbital after O_2 binding.

When considering the $3d_{xy}$ orbital, the trend is reversed. Most tetraphenyl porphyrins, with the exception of FeTPPIm-O_2, have $3d_{xy}$ orbitals that are almost doubly occupied, while the octaethyl- and unsubstituted porphyrins have occupancies closer to 1 for the same orbital. This pattern remains consistent regardless of the metal or axial

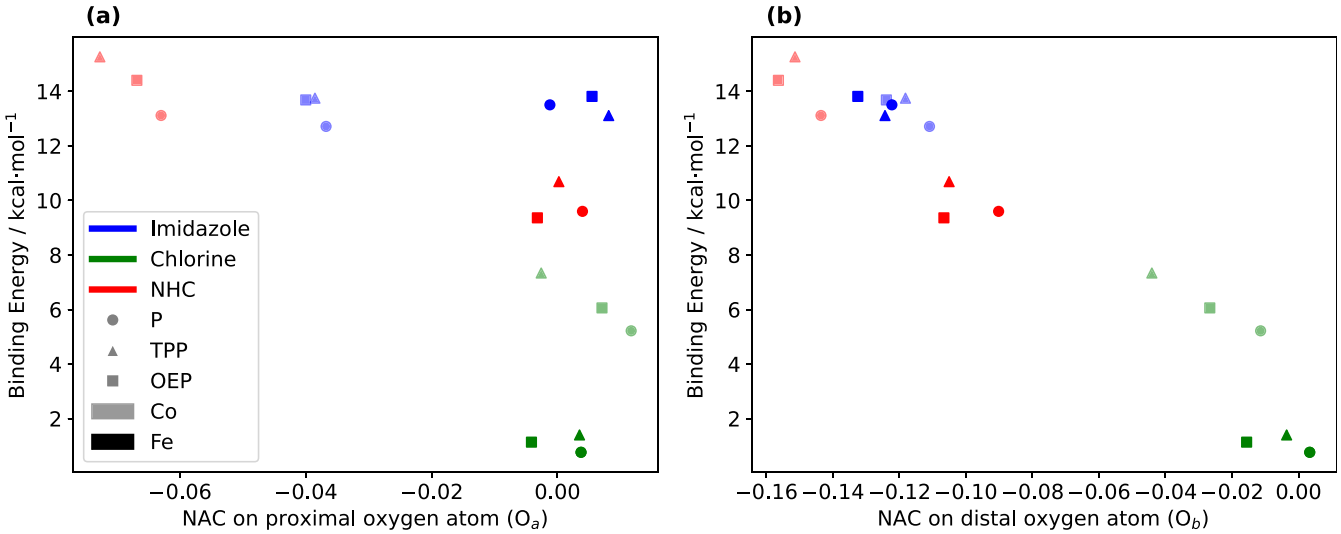

FIGURE 9 Natural atomic charge (NAC) on the proximal (A) and the distal (B) oxygen atom (horizontal axis) and their resulting binding energy to O_2. Marker color: axial ligand; marker shape: ring substituents; bold or light color: Iron or Cobalt as metal centers, respectively.

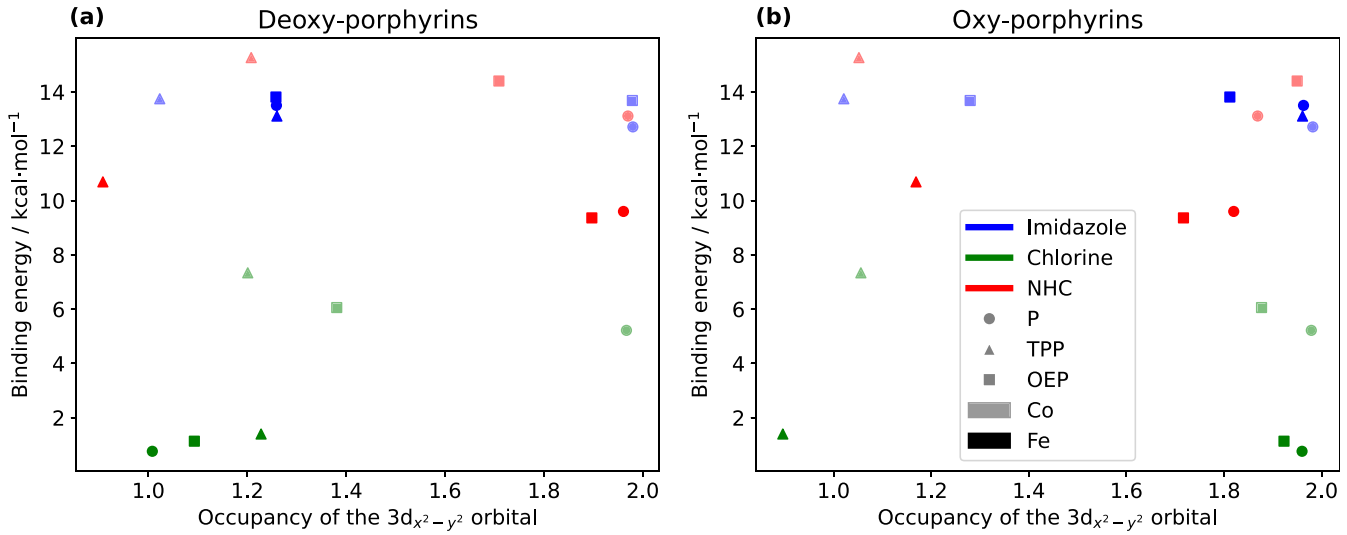

FIGURE 10 Occupancy of the 3d$_x$2–y2 orbital of the metal center in deoxy- (A) and oxy-porphyrins (B) (horizontal axis) and their resulting binding energy to O_2. Marker color: axial ligand; marker shape: ring substituents; bold or light color: iron or cobalt as metal centers, respectively.

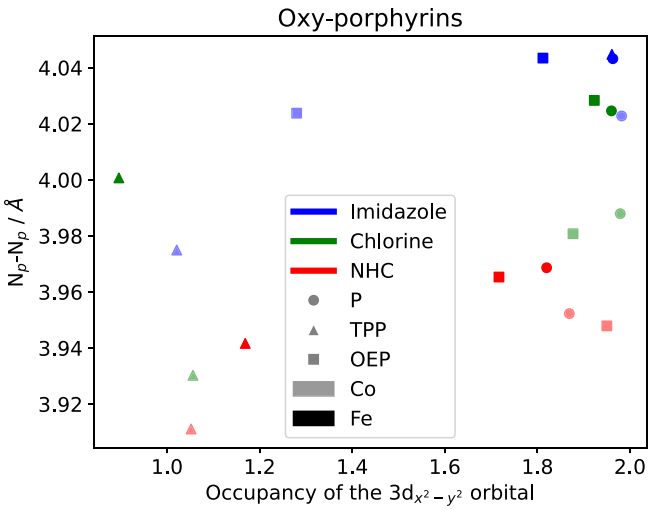

FIGURE 11 Occupancy of the 3d$_x$2–y2 orbital of the metal center in oxy-porphyrins (horizontal axis) and their average N_P–N_P distances. Marker color: axial ligand; marker shape: ring substituents; bold or light color: iron or Cobalt as metal centers, respectively.

ligand used. The singular exception of CoOEPIm is also present: upon oxygenation, the occupancy of the 3d$_{xy}$ increases.

These results align with the observed trends in geometry. Most TPP-porphyrins yield shorter N_P–N_P and M-N_P distances and exhibit larger deviations from planarity than the porphyrins with the same axial ligand. Additionally, they tend to have lower occupancy of the 3d$_x$2–y2 orbital and higher occupancy of the 3d$_{xy}$ orbital. The case of FeTPPIm-O_2, while exceptional, is also consistent in the sense that it does not follow the observed trends in orbital occupancy nor in the geometric parameters. Although establishing causality between these observations is challenging, it is evident that the geometrical differences in the TPP-porphyrins are closely related to the electronic structure of their 3d orbitals.

As for the changes, in the case of CoTPP porphyrins with NHC, the 3d$_x$2–y2 occupancy decreases by 0.156, and for CoTPP with imidazole it only decreases by 0.002. Conversely, the FeTPPNHC increased the 3d$_x$2–y2 occupancy by 0.261. The largest changes in the 3d$_x$2–y2 occupancies are obtained with chlorine and imidazole. For instance, the FePCl increases its 3d$_x$2–y2 occupancy by 0.953, while for the same porphyrin with an imidazole ligand the occupancy increases by 0.704 (Table S4).

The case for imidazole can be related to its electronic structure. Iron porphyrins with imidazole ligands tend to have a doubly- occupied 3d$_{xz}$ orbital.[21,22] Experimental work has demonstrated that histidine-coordinated deoxy-hemes tend to have two electronic structures at equilibrium, one with a double occupation of the 3d$_{xz}$ orbital, and another one with a doubly occupied 3d$_{xy}$ orbital, with the former being dominant at room temperature.[22] The iron porphyrins on this work show 3d$_{xz}$ orbitals with occupancies close to 2, and upon oxygenation an occupancy closer to 1. Conversely, 3d$_x$2–y2 orbitals on the imidazole-coordinated porphyrins start from occupancies close to 1, and change to double occupancy after O_2 binding.

Although the displacement of the metal atom could be attributed to the interaction of the 3d$_x$2–y2 orbital and nitrogen atoms of on the porphyrin ring,[22] such trend was not observed on the porphyrins in this work, either before or after oxygenation, as the displacements decrease for all the porphyrins even when the occupancy of 3d$_x$2–y2 orbitals remain closer to the value prior O_2 binding.

4 | CONCLUSIONS

The effects and interactions of different metals, axial ligands, and ring substituents on porphyrins were studied using DFT. It was observed that the choice of axial ligand significantly affects the spin state and oxygen affinity of porphyrins. Remarkably, NHC enhances the affinity

of cobalt porphyrins over that of iron porphyrins with imidazole and chlorine as axial ligands. Cobalt porphyrins coordinated to NHC have higher binding energies than other configurations, indicating the potential utility of cobalt-NHC complexes in O_2-related applications.

Furthermore, imidazole appeared to have a stabilizing effect on the porphyrin structure. Imidazole reduced the variability of geometrical parameters, irrespective of the metal or ring substituent used. A good example of this stabilizing influence was observed in the iron tetraphenyl porphyrin with imidazole (FeTPPIm), which displayed enhanced planarity in its deoxy ($RMSE_{plane} = 0.028$) and oxy-form ($RMSE_{plane} = 0.027$) compared to its cobalt counterpart in the deoxy form ($RMSE_{plane} = 0.224$), as well after O_2 binding ($RMSE_{plane} = 0.303$). Surprisingly, imidazole-coordinated porphyrins showcased consistent affinities to O_2, underlining the robustness of this ligand's stabilizing effect across various metal and substituent combinations. This stability is likely to be a factor influencing the natural selection of histidine as the axial ligand in hemoglobin. Notably, the n-heterocyclic carbene (NHC) as an axial ligand induced a low-spin state in iron deoxy-porphyrins and a triplet state upon O_2 binding, with binding energies averaging 3.6 kcal mol^{-1} lower than iron porphyrins (FeP) with imidazole. Conversely, cobalt porphyrins (CoPs) coordinated to NHC maintained a doublet (LS) configuration post-oxygenation. When chlorine was used as an axial ligand, CoPs yielded a triplet (IS) ground state. The tetraphenylporphyrins (TPP) had $3d_x2–y2$ orbitals close to singly occupied, and did not change upon O_2 binding, as the other porphyrins and the FeTPPIm, which change to a doubly occupied $3d_x2–y2$. Similarly, the TPP exhibited doubly occupied $3d_{xy}$ orbitals before and after binding O_2, whereas for the other porphyrins this orbital appears to be singly occupied. Once more, The FeTPPIm shows as an exception, as the $3d_{xy}$ orbital of this porphyrin had an occupation closer to 1.

In summary, the results emphasizes the multifaceted nature of porphyrin interactions. Although the axial ligand exerts a significant influence on the structure of the porphyrin and its affinity to O_2, the specific combination of metals, ring substituents, and axial ligands yield different results. The enhancement of the affinity of cobalt porphyrins with n-heterocyclic carbenes is worth exploring for oxygen transport and catalysis applications. Furthermore, it was shown that it is possible to tailor the porphyrins for a specific application, and in the case of their affinity to O_2, it could be modulated in increments as low as 1 kcal mol^{-1}, and in a range of 1–15 kcal mol^{-1}.

ACKNOWLEDGMENTS

The financial support from the Natural Sciences and Engineering Research Council of Canada (NSERC) Discovery grant and the Canada Research Chair Program are greatly appreciated.

CONFLICT OF INTEREST STATEMENT

The authors declare no conflict of interest.

DATA AVAILABILITY STATEMENT

The data that support the findings of this study are available from the corresponding author upon reasonable request.

ORCID

Sebastian Ovalle https://orcid.org/0000-0002-4566-2740
Cecile Malardier-Jugroot https://orcid.org/0000-0003-4785-9878

REFERENCES

[1] K. M. Adams, P. G. Rasmussen, S. W. Robert, K. Hatano, *Inorg. Chem.* **1979**, *18*, 1892.
[2] J. T. Landrum, K. Hatano, W. R. Scheldt, C. A. Reed, *J. Am. Chem. Soc.* **1980**, *102*, 6729.
[3] W. R. Scheidt, M. G. Finnegan, *Acta Crystallogr. C* **1989**, *45*, 1214.
[4] R. H. Crabtree, *The Organometallic Chemistry of the Transition Metals*, 5th ed., John Wiley \& Sons, New York, NY **2009**.
[5] K. P. Kepp, *Coord. Chem. Rev.* **2017**, *344*, 363.
[6] Y. Sun, H. Xingbang, H. Li, A. F. Jalbout, *J. Phys. Chem. C* **2009**, *113*, 14316.
[7] M. S. Liao, M. J. Huang, J. D. Watts, *J. Phys. Chem. A* **2010**, *114*, 9554.
[8] V. E. J. Berryman, M. G. Baker, R. J. Boyd, *J. Phys. Chem. A* **2014**, *118*, 4565.
[9] L. Wei, Y. She, Y. Yanmin, X. Yao, S. Zhang, *J. Mol. Model.* **2012**, *18*, 2483.
[10] J. Xiao, R. Golnak, K. Atak, M. Pflüger, M. Pohl, E. Suljoti, B. Winter, E. F. Aziz, *J. Phys. Chem. B* **2014**, *118*, 9371.
[11] T. Karpuschkin, M. M. Kappes, O. Hampe, *Angew. Chem. Int. Ed.* **2013**, *52*, 10374.
[12] X. Wang, S. Li, L. Zhao, X. Chunming, J. Gao, *Chin. J. Chem. Eng.* **2020**, *28*, 532.
[13] R. J. Cheng, P. Y. Chen, T. Lovell, T. Liu, L. Noodleman, D. A. Case, *J. Am. Chem. Soc.* **2003**, *125*, 6774.
[14] J. P. Collman, J. I. Brauman, K. M. Doxsee, T. R. Halbert, S. E. Hayes, K. S. Suslick, *J. Am. Chem. Soc.* **1978**, *100*, 2761.
[15] K. Kano, H. Kitagishi, C. Dagallier, M. Kodera, T. Matsuo, T. Hayashi, Y. Hisaeda, S. Hirota, *Inorg. Chem.* **2006**, *45*, 4448.
[16] J. P. Collman, F. Lei, *Acc. Chem. Res.* **1999**, *32*, 455.
[17] J. Li, B. C. Noll, A. G. Oliver, A. Guillermo Ferraudi, W. Graham Lappin, R. Scheidt, *Inorg. Chem.* **2010**, *49*, 2398.
[18] M. Albrecht, P. Maji, C. Häusl, A. Monney, H. Müller-Bunz, *Inorg. Chim. Acta* **2012**, *380*, 90.
[19] K. P. Jensen, U. Ryde, *ChemBioChem* **2003**, *4*, 413.
[20] J. Zhao, Q. Peng, Z. Wang, X. Wei, H. Xiao, W. Qi, H. L. Sun, F. Ma, J. Zhao, C. J. Sun, J. Zhao, J. Li, *Nat. Commun.* **2019**, *10*, 2303.
[21] H. Chuanjiang, A. Roth, M. K. Ellison, J. An, C. M. Ellis, C. E. Schulz, W. Robert Scheidt, *J. Am. Chem. Soc.* **2005**, *127*, 5675.
[22] T. Shibata, Y. Kanai, R. Nishimura, X. Liyang, Y. Moritaka, A. Suzuki, S. Neya, M. Nakamura, Y. Yamamoto, *Inorg. Chem.* **2016**, *55*, 12128.
[23] M. Kumar, M. Ansari, A. Ansari, *Spectrochim. Acta Part A: Mol. Biomol. Spectrosc.* **2023**, 284, 121774.
[24] D. J. Frisch, G. W. Trucks, H. B. Schlegel, G. E. Scuseria, M. A. Robb, J. R. Cheeseman, G. Scalmani, V. Barone, G. A. Petersson, H. Nakatsuji, X. Li, M. Caricato, A. V. Marenich, J. Bloino, B. G. Janesko, R. Gomperts, B. Mennucci, H. P. Hratchian, J. V. Ortiz, A. F. Izmaylov, J. L. Sonnenberg, D. Williams-Young, F. Ding, F. Lipparini, F. Egidi, J. Goings, B. Peng, A. Petrone, T. Henderson, D. Ranasinghe, V. G. Zakrzewski, J. Gao, N. Rega, G. Zheng, W. Liang, M. Hada, M. Ehara, K. Toyota, R. Fukuda, J. Hasegawa, M. Ishida, T. Nakajima, Y. Honda, O. Kitao, H. Nakai, T. Vreven, K. Throssell, J. A. Montgomery Jr., J. E. Peralta, F. Ogliaro, M. J. Bearpark, J. J. Heyd, E. N. Brothers, K. N. Kudin, V. N. Staroverov, T. A. Keith, R. Kobayashi, J. Normand, K. Raghavachari, A. P. Rendell, J. C. Burant, S. S. Iyengar, J. Tomasi, M. Cossi, J. M. Millam, M. Klene, C. Adamo, R. Cammi, J. W. Ochterski, R. L. Martin, K. Morokuma, O. Farkas, J. B. Foresman, D. J. Fox, *Gaussian 16, Revision B.01*, Gaussian, Inc., Wallingford, CT **2019**.
[25] S. Grimme, *J. Comput. Chem.* **2006**, *27*, 1787.
[26] F. Weigend, R. Ahlrichs, *Phys. Chem. Chem. Phys.* **2005**, *7*, 3297.

[27] S. Ovalle, C. Malardier-Jugroot, *Comput. Theor. Chem.* **2022**, *1213*, 113726.
[28] D. H. Dolphin, J. R. Sams, T. B. Tsin, K. L. Wong, *J. Am. Chem. Soc.* **1978**, *100*, 1711.
[29] M. K. Ellison, C. E. Schulz, W. Robert Scheidt, *Inorg. Chem.* **2002**, *41*, 2173.
[30] Y. Liu, X. Wei, J. Zhang, W. Fuller, C. E. Schulz, J. Li, *J. Am. Chem. Soc.* **2017**, *139*, 5023.
[31] Y. Li, J. S. Huang, Z. Y. Zhou, C. M. Che, X. Z. You, *J. Am. Chem. Soc.* **2002**, *124*, 13185.
[32] D. Manna, R. Lo, P. Hobza, *Dalton Trans.* **2019**, *49*, 164.
[33] M. E. Ali, B. Sanyal, P. M. Oppeneer, *J. Phys. Chem. B* **2012**, *116*, 5849.
[34] V. V. Smirnov, E. K. Woller, S. G. DiMagno, *Inorg. Chem.* **1998**, *37*, 4971.
[35] R. D. Jones, D. A. Summerville, F. Basolo, *Chem. Rev.* **1979**, *79*, 139.
[36] Takayuki Suzuki, Yuji Soejima, Hiroyuki Nishide, Eishun Tsuchida, *Effect of an Oxygen-Binding Reaction at the Cobalt Porphyrin Site Fixed in a Polymer Membrane on Facilitated Oxygen Transport*, **1995**, *68*, 1036.
[37] T. Okamoto, K. Shudo, T. Ohta, *J. Am. Chem. Soc.* **1975**, *97*, 7185.
[38] M. H. Keyes, M. Falley, R. Lumry, *J. Am. Chem. Soc.* **1971**, *93*, 2035.
[39] A. Rossi-Fanelli, E. Antonini, *Arch. Biochem. Biophys.* **1958**, *77*, 478.
[40] M. Y. R. Wang, B. M. Hoffman, S. J. Shire, F. R. N. Gurd, *J. Am. Chem. Soc.* **1979**, *101*, 7394.
[41] D. D. Miller, R. Siriwardane, T. Simonyi, *Energy Fuel* **2011**, *25*, 4261.
[42] Y. Iimura, T. Sakurai, K. Yamamoto, *Bull. Chem. Soc. Jpn.* **1988**, *61*, 821.
[43] S. Nasri, M. Hajji, M. Guergueb, S. Dhifaoui, V. Marvaud, F. Loiseau, F. Molton, T. Roisnel, T. Guerfel, H. Nasri, *J. Mol. Struct.* **2021**, *1231*, 129676 .
[44] L. D. Sparks, J. R. Chamberlain, J. A. Shelnutt, M. S. Park, M. R. Ondrias, C. J. Medforth, M. O. Senge, K. M. Smith, *J. Am. Chem. Soc.* **1993**, *115*, 581.
[45] P. Olivier, M.-P. Faucon, in *Encyclopedia of Geochemistry: A Comprehensive Reference Source on the Chemistry of the Earth* (Ed: W. M. White), Springer International Publishing, Cham **2016**, p. 1.

SUPPORTING INFORMATION

Additional supporting information can be found online in the Supporting Information section at the end of this article.

How to cite this article: S. Ovalle, C. Malardier-Jugroot, *J. Comput. Chem.* **2025**, *46*(1), e27505. https://doi.org/10.1002/jcc.27505